D. DINESH[◯][1], A. MEGALINGAM[◯][1*]

DRY SLIDING FRICTION AND WEAR BEHAVIOUR OF LEADED TIN BRONZE FOR BEARING AND BUSHING APPLICATION

Among different bearing materials, copper-based alloys are the most important source for bearing and bushing applications. In this work, the tribological behavior of a leaded tin bronze (Cu-22Pb-4Sn) against an EN31 Steel for various loads (20 N, 70 N, 120 N) and different sliding velocity (1 m/s, 3 m/s, 5 m/s) at 3000 m sliding distance is performed using a pin on disk tribometer. Irrespective of all loads and sliding velocity, a higher specific wear rate is observed at 1 m/s and 120 N that fails to facilitate the formation of lubricating film, whereas a lower specific wear rate is evident when the sliding velocity is increased to 5 m/s. This is attributed to the formation of a stable oxide layer that has been confirmed through the Energy dispersive X-ray spectroscopy analysis and Scanning electron microscopy. The coefficient of friction is observed in reducing trend from 0.69 to 0.48 for the increasing load (70 N, 120 N) and sliding velocity (3 m/s and 5 m/s) due to stable thin oxide film formation. Also, the increase in frictional force and loading the interacting surface temperature is increased to a maximum of 102°C. The Grey relational analysis indicates that the optimal parameters for the minimum specific wear rate and coefficient of friction is 120 N and 5 m/s that has been confirmed with experimental analysis.

Keywords: Wear, coefficient of friction, Microstructure, leaded tin bronze, grey relational analysis

1. Introduction

Bronze is a copper-based alloy that exists in different types such as, manganese bronze, tin bronze, aluminum bronze, leaded bronze and silicon bronze for various engineering applications [1]. Among these alloys, tin bronze and leaded bronze are used for bearing and bushing application. It is used as a bulk material or a lining material to the steel piece to achieve moderately high strength, a high load capacity and good thermal conductivity [2-4]. Reducing wear and friction is an involved task for the failure of tribocomponents like gears, valve seats, seam fittings and piston rings which is made of bronze materials [5]. Several investigations have been focused in sliding wear behaviour of various bronzes since 1990's [6]. Leaded tin bronze is an extensively used material due to its excellent seizure resistance offered by lead [7]. A higher lead content in the leaded tin bronze which acts as a solid lubricant by smearing lead into the interacting surface with the counterpart during sliding [8,9]. The friction and wear resistance are enhanced by adding tin to this type of copper alloy [10]. Tin bronze alloy is used at a high temperature and high loading conditions. However, the machinability of such

tin bronze alloys is challenging [1]. In leaded tin bronze, the combined effect of the alloying elements lead and tin are essential to achieve the desired properties in bearing. Investigations in aluminium bronze, zinc based alloy, leaded tin bronze and bronze 663 those produced by various processes like continuous casting, centrifugal casting and sand casting in relation to wear and friction have been studied. The evaluation of different bronzes are tested under various set up like pin and ring type, pin-on-disk, ball on disk, radial journal bearing test rig and thrust bearing test rig. A leaded tin bronze (Cu-7.2Sn-7.3Pb-2.9 Zn) samples produced by casting is tested against EN25 steel using the pin on disk apparatus. It is noted that the lead particles smearing on the interacting surface fails at low sliding velocity leads to a higher wear rate and tends to form microcracking in the sub-surface. At higher sliding velocity, high frictional heating tends to reduce the microcracking by forming a stable solid lubricating film transfer layer. Also, the debris adhere to the interacting surface which improves the wear resistance [11]. At low sliding speed, Zinc based alloy that are rich in aluminium and zinc shows superior wear rate when compared to aluminium bronze and leaded tin bronze. This is due to the presence of α and η mi-

[1] BANNARI AMMAN INSTITUTE OF TECHNOLOGY, DEPARTMENT OF MECHANICAL ENGINEERING, SATHYAMANGALAM, ERODE-638401, TAMILNADU, INDIA

* Corresponding author: mechmega@gmail.com

croconstituents in which in which η is lubricating in nature [12,13]. Aluminium bronze has excellent compressive strength and hardness, it shows inferior wear rate at lower sliding speed when compared to leaded bronze and superior wear rate than zinc based alloy [14]. Addition of alloying element, manganese in the leaded tin bronze (Cu-2.37Pb-5.55Sn-0.226 Mn) has an adverse effect on improving the fatigue resistance due to presence of Mns phase in the matrix. But the loss of weight of sample occurs at higher rate which forms deep grooves on the surface [2]. The effect of phosphorous which forms the Cu_3P phase surrounds the (Zn-Cu)S phase that prevents the growth, increases tensile strength and its fatigue strength but the weight loss due to friction is high [15]. The investigation under dry and lubricated conditions of copper tin lead alloy (6 wt% tin and 0, 5, 10, 15, 20 and 25 wt% lead and 15 wt% lead and 0, 3, 6, 9, 12 and 15 wt% tin) with fine lead structure and coarse lead structure are produced by chill cast and sand cast respectively. In the dry condition testing, the addition of lead upto 10% and tin upto 3% have shown a reducing effect in relation to the coefficient of friction. It also observed that there is no distinction behaviour found in the coarse and fine leaded structure. In case of lubricated condition, the sand cast alloy performance is better than that of the chilled cast alloy. The paraffin oil of alloy with 15% lead and 3% tin shows low wear rate when compared to ethyl alcohol and thin paraffin. When the experiments are performed on various compositions of these alloys, it is found that Cu-3Sn-10Pb with coarse distribution is favorable in reducing the friction and wear under both lubricated and unlubricated condition [16]. The frictional mechanism of Cu-3Sn-10Pb alloy and unleaded bronze (Cu-Sn8) found that the coefficient of friction is low for the leaded bronze and high for the unleaded alloy. Accordingly, the wear rate is higher for the leaded bronze and lower for the other graded materials. Hence, two distinctive wear behaviour was observed. Firstly, lead rich layer is smeared on to the surface forms lead oxide layer which tends to act as a lubricant to increases the wear resistance. Secondly, the particles of lead and copper are detached from the base metal to form the third body wear process [3]. It has been noticed that leaded tin bronze produced by powder metallurgy route further coated with ZrO_2 by HVOF spraying technique that has been tested in the real type internal combustion engine for 500 hours. It is found that the hard particle ZrO_2 is embedded into the soft matrix which forms the cavities and pores in the surface. It reduces the abrasion damage and lowers the frictional losses [17]. Then, bronze 663 with various composition of graphite of 4.5% without nickel coated and 11.7%, 15%, 18.3% with nickel coated is produced through powder metallurgy route. It is found that graphite of uncoated nickel tends to have poor interfacial bonding with the matrix material. But the 15% nickel coated graphite composites produce mechanically mixed layer that tends to have higher specific wear rate, high hardness and higher friction coefficient [18,19]. In addition to the above investigations, a special attempt of copper composites with lubricating phase particles like MoS_2, WS_2, graphite and glassy carbon of 5 to 20% produced by stir casting and powder metallurgy route. The improved wear resistance is found in graphite and tungsten

disulphide [20]. Recently, the friction reduction of engine bearing of copper based alloy by various coating has been addressed [21].

Leaded tin bronze (Cu-22Pb-4Sn) alloy used for bearing that failed at high load condition. In order to address this issue, this research work is mainly focused on the influence of lead in relation to microstructure features of worn surface. Also, temperature effects and tribological properties like specific wear rate and coefficient of friction at a higher load has been studied using pin on disk tribometer.

2. Experimental details

2.1. Working material

In this investigation, the leaded tin bronze (Cu-Pb24-Sn4) alloy is prepared by a centrifugal casting and solidified by natural convection. The chemical composition of the matrix material is given in Table 1.

TABLE 1

Composition details of the leaded tin bronze material in wt%

Cu	Sb	P	Ni	Fe	Zn	Pb	Sn
71.25	0.095	0.004	0.24	0.18	0.34	23.77	4.1

2.2. Friction and wear test

Tribological behaviour of leaded tin bronze alloy was studied by considering the process parameters such as load, sliding velocity and sliding distance. The control parameters used in this process and their levels are listed in Table 2. The cast samples specimen was machined and prepared to 10 mm square. The samples are cleaned with acetone and dried before conducting friction and wear test. Pin on disk tribometer was used to investigate the dry sliding wear behavior of leaded tin bronze against EN31 hardened steel disk of 60 HRC as per the standard ASTM G99 as shown in Fig. 1. Each experiment was performed with three sets of trials at room temperature to analyze the experimental results.

TABLE 2

Control Parameters and levels

Level	Applied Load (L) (N)	Sliding Velocity (v) (m/s)	Sliding distance (D) (m)
1	20	1	3000
2	70	3	3000
3	120	5	3000

During the conduct of each experiment, the interacting surface temperature was recorded using thermal image camera and mass loss of the every sample was calculated by weighted down before and after the test by using a weigh balance of 0.0001 g accuracy (Δm = Weight before wear – Weight after wear)
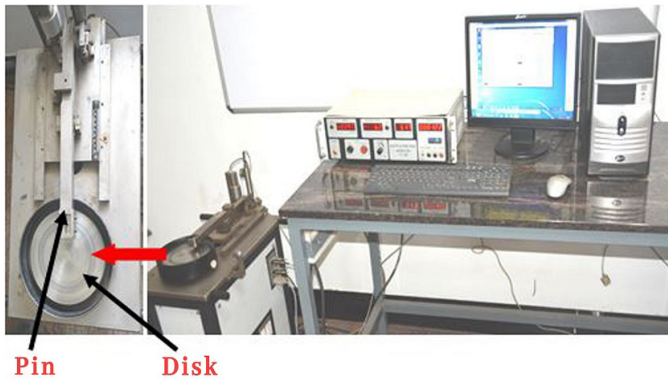
Fig. 1. Pin on Disk Experimental Set Up

The specific wear rate and coefficient of friction are calculated using the Eq. (1) and Eq. (2):

$$\text{Specific wear rate (SWR)} = \frac{\Delta m}{\rho \times Fn \times D} \quad (1)$$

Coefficient of friction (COF) =

$$= \text{Frictional force /Applied Load} \quad (2)$$

The worn surface of samples was analyzed using Scanning Electron Microscope (SEM) and Energy Dispersive X-Ray spectroscopy (EDX) to understand the wear mechanism. The optimal parameter for the low SWR and COF was determined using multiresponse-Grey Relational Analysis (GRA). Then, confirmation experiments were conducted to validate the results.

3. Result and discussion

3.1. Microstructure

Specimens are cut from the casting with size of Ø20×10 mm, which are mounted using the specimen mounting press. Further, the surfaces of the samples are mechanically ground with various abrasive grit papers in sequence followed by fine polishing with 1μm diamond paste and chemically etched with potassium dichromate ($K_2Cr_2O_7$) solution. The SEM micrograph of the leaded tin bronze alloy is shown in Fig. 2. The dendritic morphology is evident with lead as discrete particles represented in Fig. 2a and primary α–Cu and intermetallic compound Cu-Sn is marked as shown in Fig. 2b.

Fig. 2. Microstructural observation of leaded tin bronze a) at Lower Magnification at 250×, b) at Higher Magnification at 1000×
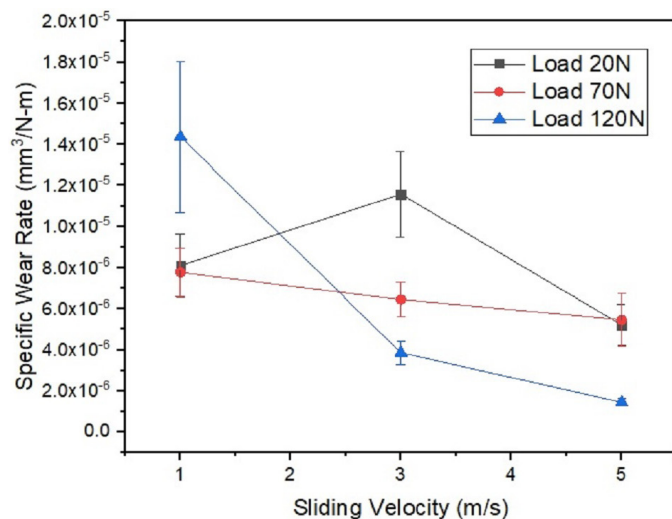
Fig. 3. Effects of applied load and sliding velocity on specific wear rate

3.2. Effect of applied load and sliding velocity on specific wear rate

In leaded tin bronze, the discrete particles of lead do not have good metallurgical compatibility with the matrix material [11]. Also, the microcracking phenomenon occurs at a low sliding speed that causes a high wear rate in all types of leaded copper alloy [21]. In addition to these inferences, Fig. 3 depicts the relationship between the applied load and sliding velocity concerning to specific wear rate during the sliding wear behavior at a high sliding distance of 3000 m.

At a load of 20 N and 1m/s, the intermediate SWR that occurs as shown in Fig. 3. The SEM micrographs of the worn out surface of leaded tin bronze contains shallow grooves, which is parallel to the direction of sliding can be observed in Fig. 4a. In addition to this, the microcracks that occurred in the copper
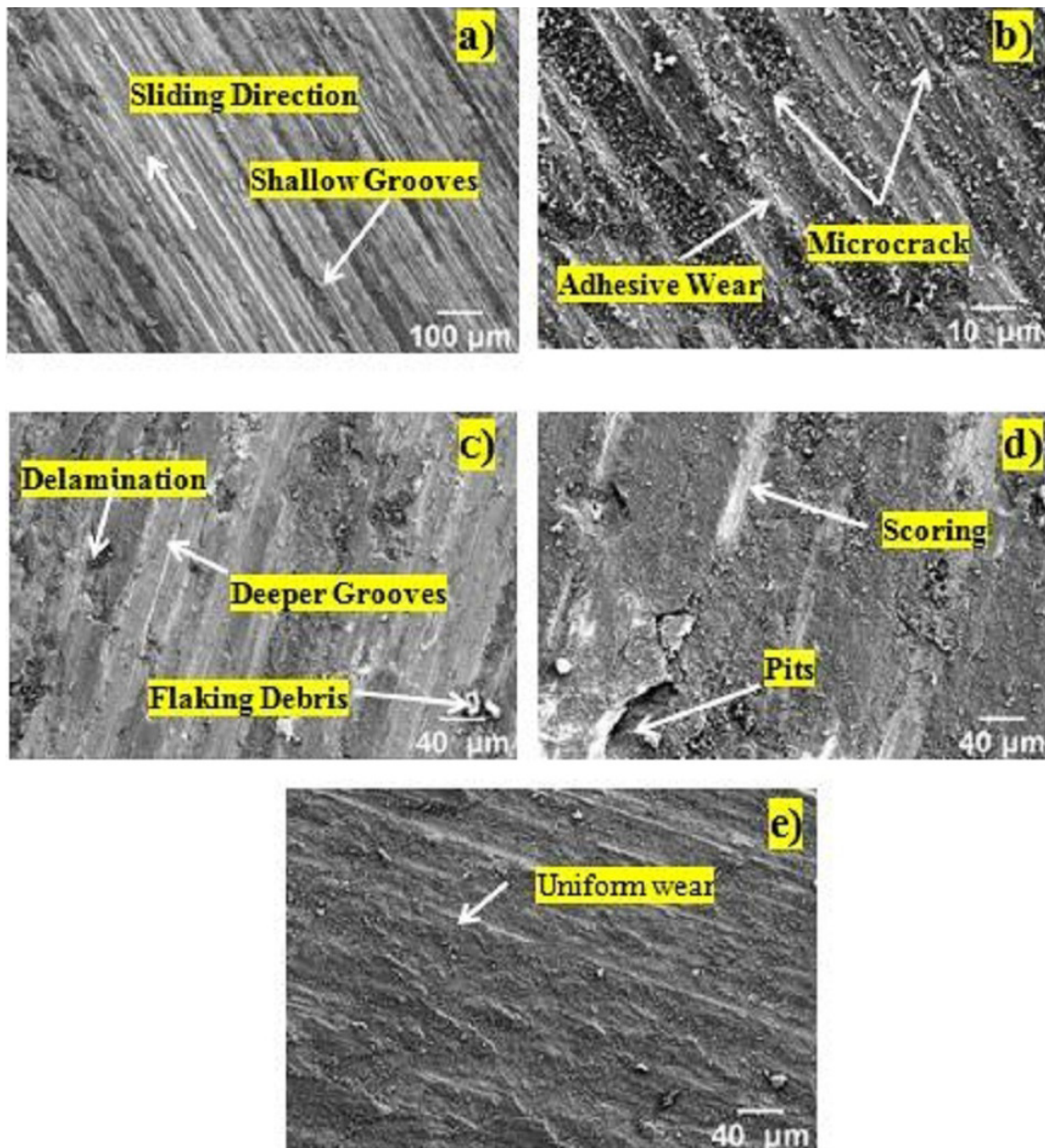
Fig. 4. SEM Picture after sliding, the worn out surface of the leaded tin bronze alloy at 20 N with sliding velocity a) and b) at 1 m/s, c) and d) at 3 m/s, e) at 5 m/s

lead interfacial region have not increased the SWR because the lead particles removed from the wear track and gets smeared onto the mating surface which results in adhesive wear on the worn surface is indicated by an arrow mark in Fig. 4b. When increasing the sliding velocity from 1 m/s to 3 m/s, a high SWR occurs due to the change in mode of wear mechanism from adhesive to abrasive. It means that the two surfaces form an intimate contact with each other that has been deformed plastically, inducing deeper grooves, scoring with bright marks and pits as shown in Fig. 4c. and Fig. 4d. Thus, the tendency of microcracking occurs at a lower sliding velocity leading to delamination when sliding velocity increases. It is also observed that the lead particles of the alloy failed to form the lubricating flim, instead it gets smeared out from the matrix forming coarse flaking debris represented in Fig. 4c. The abrasive wear mechanism plays a significant role

in increasing the SWR. Further increase in sliding velocity to 5 m/s, the SWR decreases due to the lead particles in the alloy get smeared into the contacting surface forms a stable lubricating flim. It is also evident that uniform wear occurs is represented in Fig. 4e forms an adhesive wear.

From Fig. 3, the low SWR is observed at 70 N and 1 m/s, but it is intermediate at 3 m/s and 5 m/s. When the sliding velocity is at 3 m/s, the dispersion of lead particles from the base material over the mating surface occurs during sliding. The accumulation of ejected particles occurs at a faster rate tends to form a stable lubricating film layer on the surface that results in adhesive wear shown in Fig. 5a. This results in reducing the material damage and also the wear debris is observed on to the surface as shown in Fig. 5a. At 5 m/s, the smearing of lead formation occurs in reducing the microcrack propagation along with the
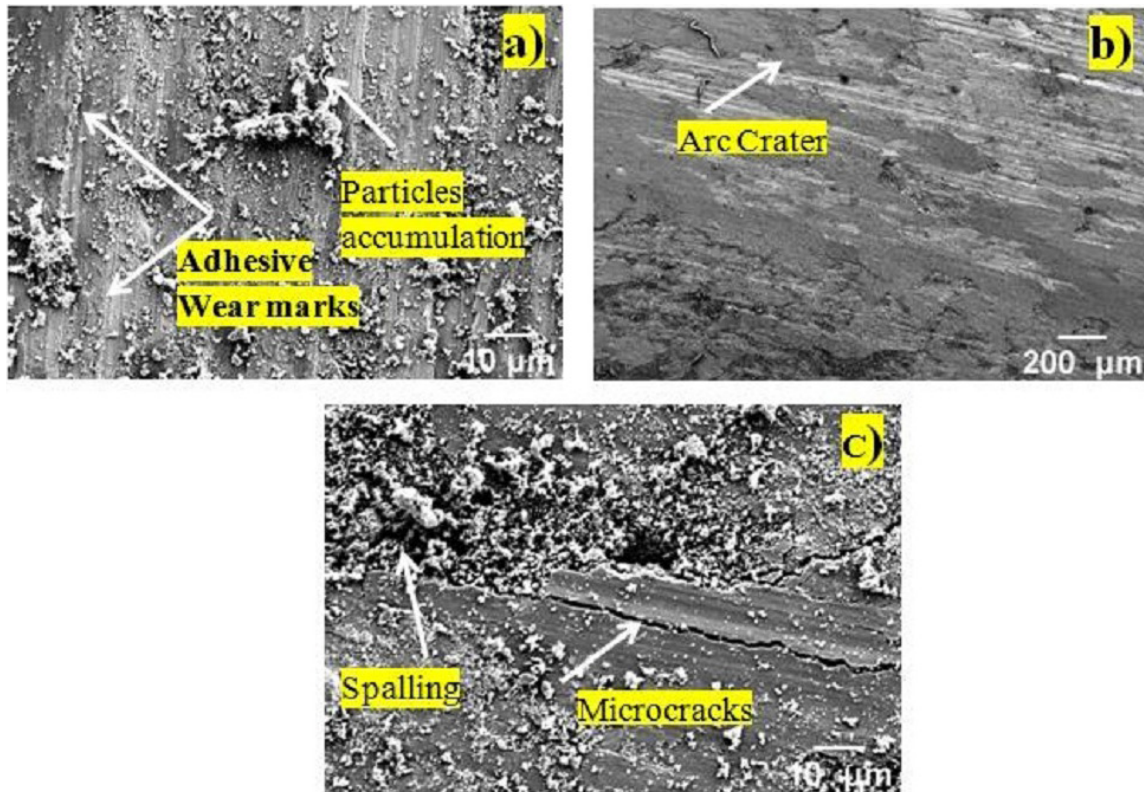
Fig. 5. Worn surface micrographs of copper based alloy of 70 N a) at 3 m/s, b) & c) at 5 m/s

surface results in the effect of spalling indicated in Fig. 5c. It also forms an arc crater that confirms the third body wears as shown in Fig. 5b.

In Fig. 3, at 120 N and 1 m/s, high SWR is observed and a low SWR is attained while increasing the sliding velocity to 3 m/s and 5 m/s. The SEM micrographs of the worn out surface at 1 m/s is shown in Fig. 6a. The EDX analysis shows Cu peaks is higher than Fe and significant amount of Pb and Sn peaks as shown in Fig. 7. It reveals that the material is transferred between a pin and counterface during sliding. A higher Cu peaks implies that the material is transferred from the counterface to the pin which results in adhesive wear marks on the surface as shown in Fig. 6a. It also indicates that deeper groove marks on the surface is occurs due to the softer material lead smeared out from the matrix material copper that fails to form the lubricating film which causes abrasion. The stable oxide layer has occurred in relation to the phase diagram of Cu-O at 5 m/s as indicated in Fig. 6b. The EDX analysis of the worn out surface is indicated in Fig. 8a is line mapping analysis. From Fig. 8c shows Fe peak is higher than the copper which shows that transfer of Fe particles from the counterface to the pin that occurs in between the contacting surfaces. In addition, Fig. 8b confirms that the element of oxygen forms a stable transfer with all element of this alloy that has been observed, which leads to a mechanically mixed layer that significantly reduces the SWR. Fig. 9a and 9b show the area chosen for analysis and the corresponding elemental mapping respectively. Fig. 9c shows the presence of Cu element is lesser and the dispersion of alloying elements Fe, Pb, Sn, Cr, and C which confirms the oxide layer formation that reduces the SWR.
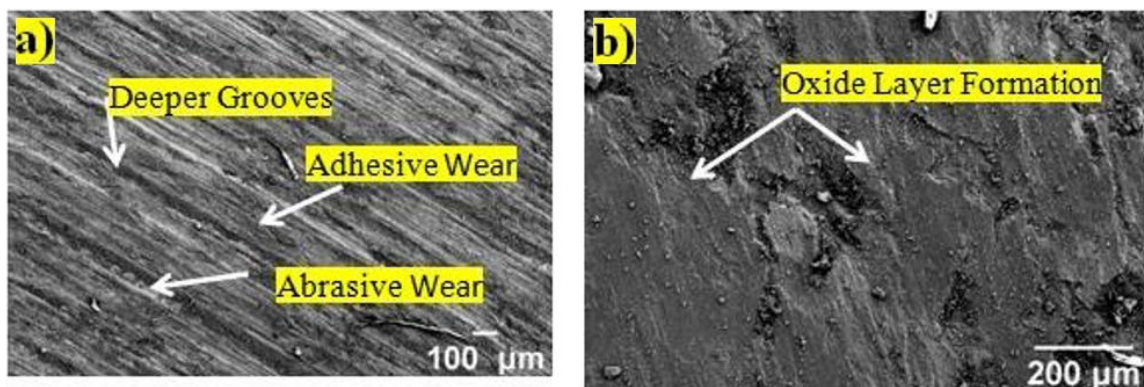

Fig. 6. SEM Microstructure of wear surface at 120 N a) at 1 m/s, b) at 5 m/s
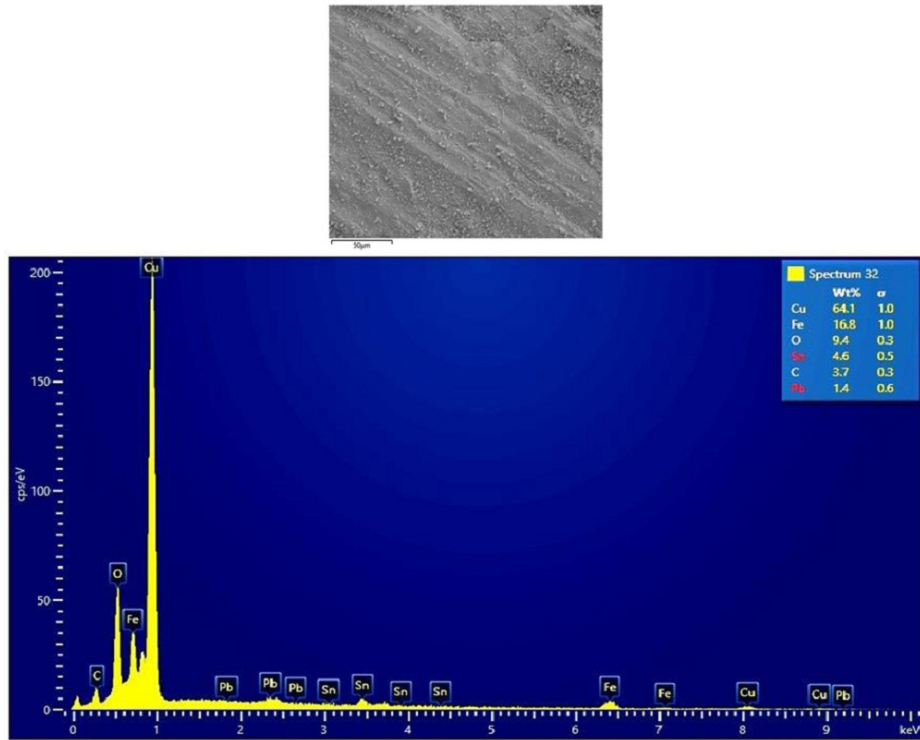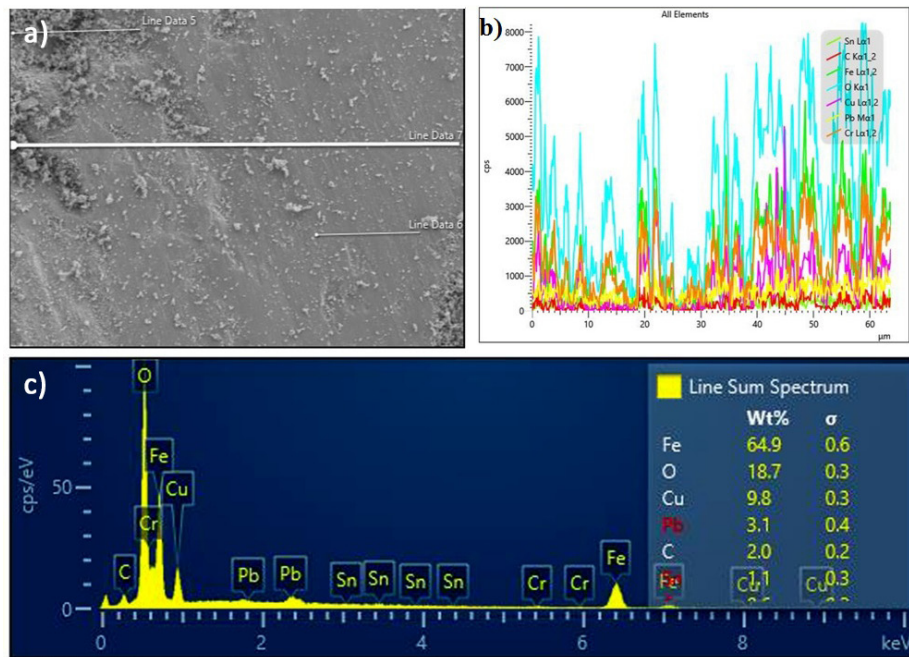
Fig. 7. EDX Analysis of 120 N at 1 m/s

Fig. 8. EDX Analysis of 120 N at 5 m/s a) Chosen for analysis by line mapping, b) Individual mapping of Elements, c) worn out surface analysis

3.3. Effect of Applied Load and Sliding velocity on coefficient of friction

Fig.10 reveals the relationship between the applied load and sliding velocity on the coefficient of friction (COF). The COF decreases with increase in applied loads of 70 N and 120 N. It happens due to the accumulation of lead particles at a faster rate and the mechanically mixed oxide layer forms a stable transfer layer on the wear surface that reduces the COF accordingly. This similar behaviour was observed in M. Kestursatya et.al [22]. At 20 N, the COF increases when the sliding velocity increases to 3 m/s. This is due to the failure of the stable lubricating film of lead. Further, the COF decreases at 20 N and 5 m/s, because the interaction between the two surfaces forms an adhesive wear. Minimum COF of 0.30 was observed at 120 N and 5 m/s during the dry sliding wear behavior process.
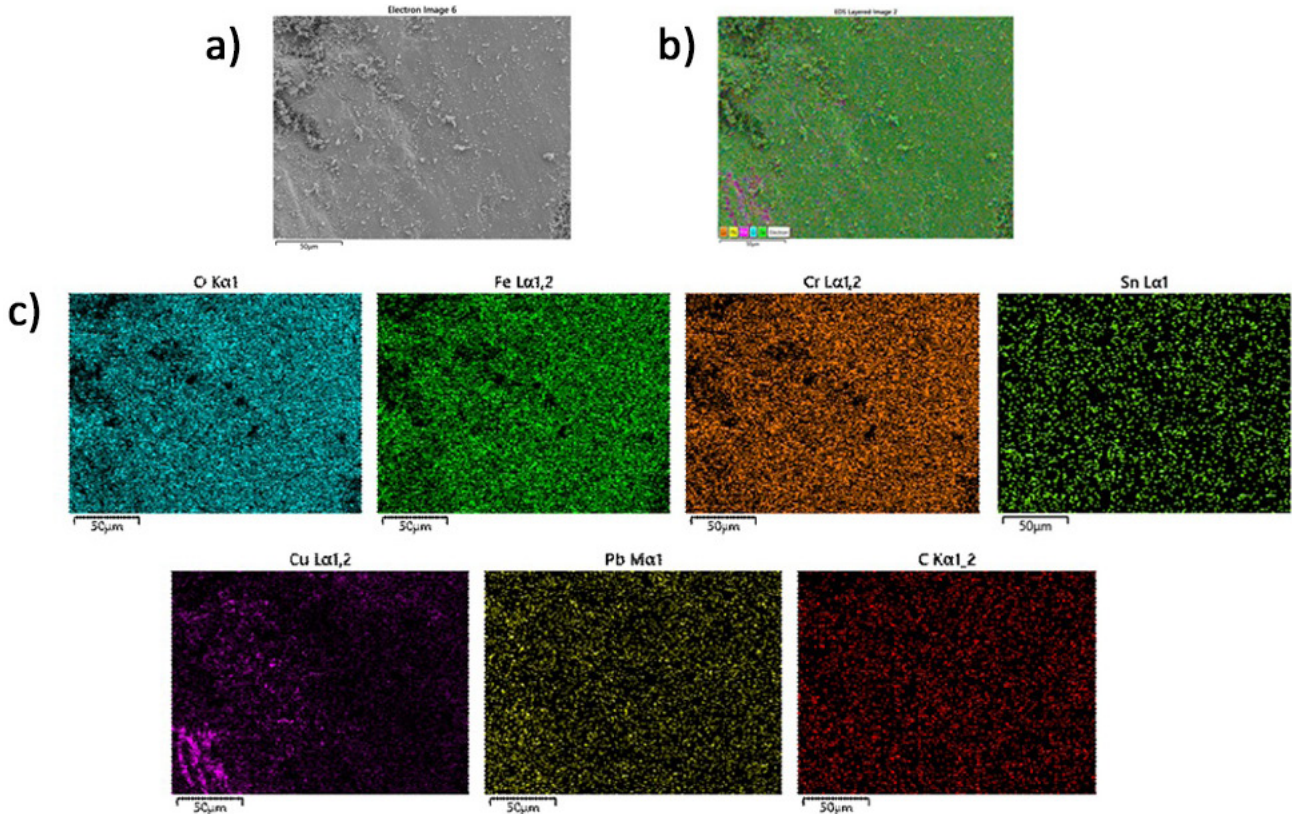
Fig. 9. Elemental mapping of worn surface at 120 N and 5 m/s, a) Chosen area for analysis, b) Consolidated map of elements, c) Dispersion of elements
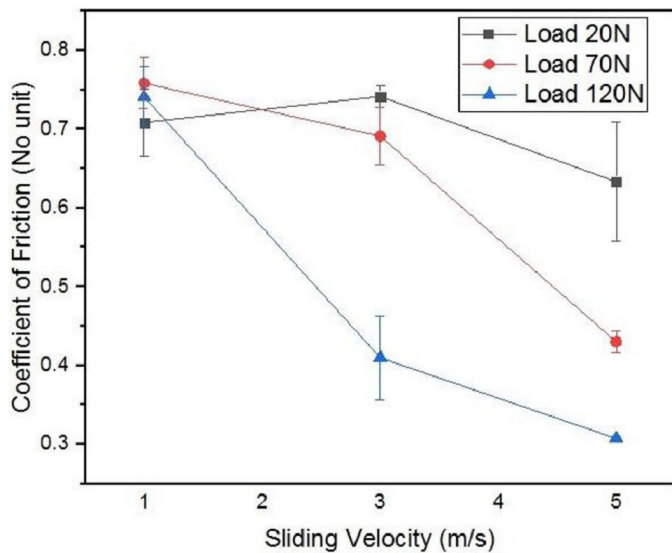

Fig. 10. Effect of applied load and sliding velocity on Coefficient of friction

3 m/s, 5 m/s) as shown in Fig. 11. In general, the frictional heating increases linearly with the test duration. In Fig. 11a for the sliding velocity 1 m/s, the temperature increases with increase in applied load for the test duration. It was observed for the load of 70 N, the temperature is slightly lower when compared to 20 N. This specifies a non uniform contact of specimen surface during the sliding results in increase of COF. Further increase in the test duration, results in proper surface contact between two asperities to form the adhesive wear that reduces the specific wear rate. In Fig. 11b at 3 m/s, an increasing trend in temperature was noted at various loads. An average temperature of 102°C was recorded for the load of 120 N, which increases the frictional heating causing the lubricating film forms the stable transfer oxide layer reduces the SWR at 5 m/s. But, the rate of increase in temperature was lower at 20 N and 70 N as shown in Fig. 11c. The thermal image of maximum temperature during the experiment was recorded as shown in Fig. 11d for the load and sliding velocity 120 N and 5 m/s respectively.

3.4. Effect of temperature near the mating surface during sliding

The temperature near the surface of the pin specimen has been recorded using a FLIR thermal imaging camera. The readings are plotted as a function of temperature and test duration, for the loads (20 N, 70 N, 120 N) and sliding velocity (1 m/s,

3.5. Grey Relational Analysis –Multiresponse Characteristics

The grey means the primal data with poor, incomplete or undetermined information. The relation with the incomplete information and complex is called Grey relation. The primary objective of GRA is to obtain the optimum parameters for the
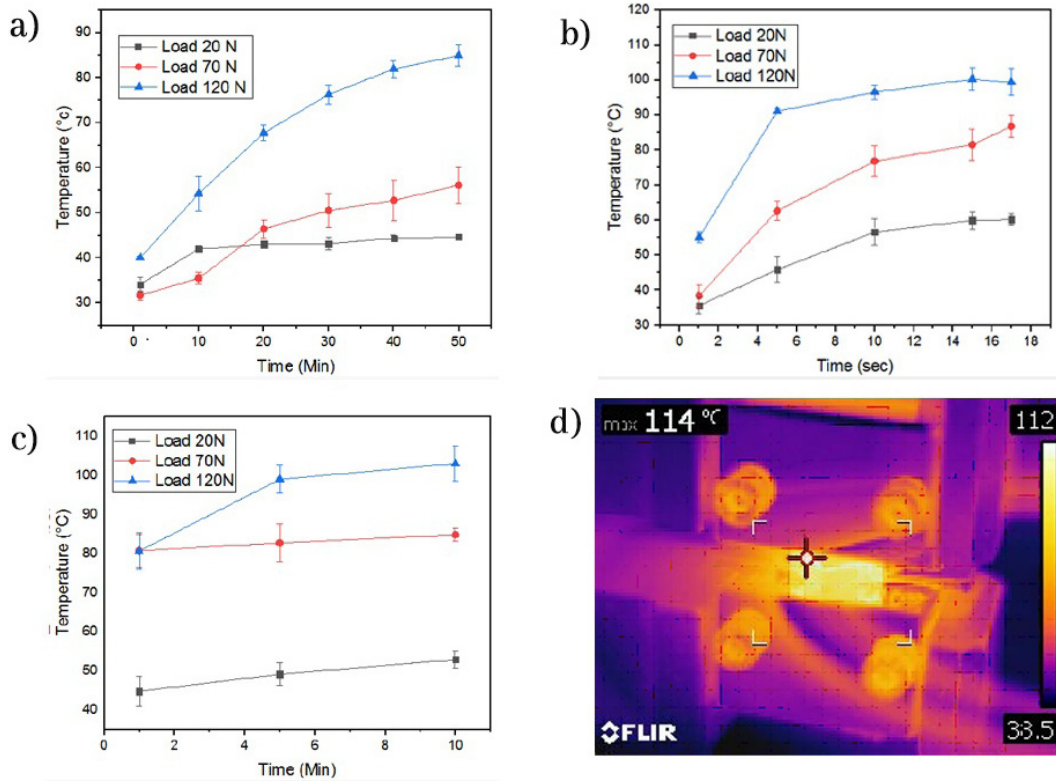
Fig. 11. Effect of temperature near the mating surface a) at 1m/s, b) at 3 m/s, c) at 5 m/s, d) Experimental reading at 120 N and 5 m/s

improved SWR and COF. The experiments consist of nine tests with three experimental trials performed with influencing parameters like applied load, sliding velocity and sliding distance of 3000 m. Table 3 shows the experimental results for SWR and COF, where analytical processing steps is to be performed using GRA are discussed below as follows.

TABLE 3

Design of experiments and its results

Exp. no.	Design Parameters			Experimental Results	
	Load	Sliding Velocity	Sliding Distance	Specific wear rate	Coefficient of Friction
	N	m/s	m	mm^3/Nm	(No unit)
1	20	1	3000	8.10185E-06	0.7085
2	20	3	3000	1.15741E-05	0.7416667
3	20	5	3000	5.20833E-06	0.6333333
4	70	1	3000	7.77116E-06	0.7585714
5	70	3	3000	6.44841E-06	0.6914286
6	70	5	3000	5.45635E-06	0.43
7	120	1	3000	1.43711E-05	0.7411111
8	120	3	3000	3.85802E-06	0.4097222
9	120	5	3000	1.44676E-06	0.3072222

Step 1: **Data Preprocessing and Normalizing:** The pre-processing of data used in grey analysis is done for another analysis by normalizing the data. Data normalizing is the process of converting the original sequence into decimal sequence between 0 and 1. In this study, the expected data sequence is in the form of Lower the better was selected for SWR and COF.

Table 4 illustrates the normalized values which indicate the situation of better characteristics.

TABLE 4

Normalized Experimental Results

Exp. no.	SWR	CoF
1	0.485	0.111
2	0.216	0.037
3	0.709	0.277
4	0.511	0.000
5	0.613	0.149
6	0.690	0.728
7	0.000	0.039
8	0.813	0.773
9	1.000	1.000

Step 2: **Deviation sequence:** It is resolute by finding the difference between the reference sequence and the comparability reference.

Step 3: **Grey Relation Coefficient (GRC):** Calculated Grey relation coefficient is to obtain the connection between the ideal and the actual normalized experimental results. Also ζ, is an identification coefficient that lies in between 0 and 1. $\zeta = 0.5$ is also widely accepted.

Step 4: **Grey Relational Grade (GRG):** Grey relational grade is the average of the grey relation coefficient if 0.5 is selected. It also gives us the relation between the comparability and reference sequences. Table 5 shows the calculated GRC and GRG in order.

TABLE 5

Calculated GRC and GRG Values and Rank

Exp. no.	GRC		GRG	Rank
	SWR	CoF		
1	0.493	0.360	0.426	6
2	0.390	0.342	0.366	8
3	0.632	0.409	0.521	4
4	0.505	0.333	0.419	7
5	0.564	0.370	0.467	5
6	0.617	0.648	0.632	3
7	0.333	0.342	0.338	9
8	0.728	0.688	0.708	2
9	1.000	1.000	1.000	1

Step 5: **Analysis results of GRG for optimal parameters:** In accordance to Table 5 and Fig. 12 represents the GRG value for the performed experimental design. It clearly indicates that experiment 9 has the highest GRG among the nine experiments. In this experiment the indicating coefficient is taken as 0.5 and GRG is 1.00. Thus, this indicates the relationships among the sequence are identical. The optimum parameters 120 N at 5 m/s are obtained which improves the SWR and COF.

Step 6: **Conducting confirmation experiment:** The predicted and calculated values for the output responses of SWR and COF are obtained with 6.92% and 3.33% error respectively. It determines that error values that lie within the satisfactory level of less than 10%.
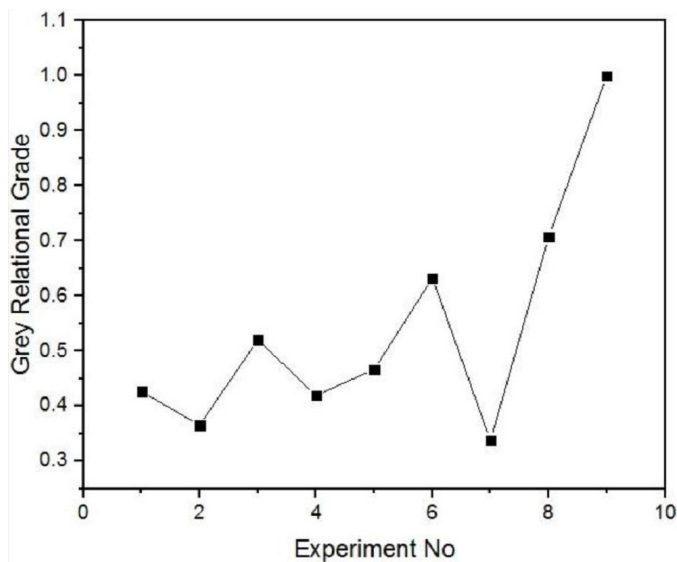

Fig. 12. Graph of Grey relational Grade

4. Conclusion

The wear performance of leaded tin bronze loaded against the EN31 steel disk lead to the following conclusion:

1. Low SWR of (1.44×10^{-6} mm^3/N-m) was observed at the dry sliding condition of 120 N and 5 m/s. At an axial load of 20 N, a significant increase of 42.8% in SWR was ob-served with an increasing sliding velocity from 1 m/s to 3 m/s. However, SWR decreased by 55.05% with increase in sliding velocity from 3 m/s to 5 m/s respectively.

2. At 120 N, SWR decreases to 73.5% and 62.5% by raising the velocity from 1 to 3 m/s and at 70 N the decreasing trend of SWR is observed to be 17.11% and 14.75 % by raising the velocity from 3 m/s to 5 m/s.

3. COF decreases upto 22.58% upon increasing the load and sliding velocity. At 20 N, the COF is increased by 5.3% when the sliding velocity is increased from 1 m/s to 3 m/s but 17.42 % decrease in COF occurs when the sliding velocity rise from 3 m/s to 5 m/s.

4. Increase in frictional force increases the temperature at all applied loads and test duration. The highest temperature of 102°C at 120 N and 5 m/s was observed.

5. GRA indicates that the optimal parameters for the minimum SWR and COF is 120 N at 5 m/s. Computational results are in correlation with the experimental results.

REFERENCES

[1] R.F. Schmidt, D.G. Schmidt, (10Ed.), Selection and application of copper alloy castings: Metals Handbook, ASM International, USA (1993).

[2] H. Turhan, M. Aksoy, V. Kuzucu, M.M. Yildirim, J. Mater. Process. Technol. **114** (3), 207-211 (2001). DOI: https://doi.org/10.1016/S0924-0136(01)00569-6

[3] S. Equey, A. Houriet, S. Mischler, Wear. **273** (1), 9-16 (2011). DOI: https://doi.org/10.1016/j.wear.2011.03.030

[4] G.C. Pratt, Powder Metall. **12** (24), 356-385 (2014). DOI: https://doi.org/10.1179/pom.1969.12.24.007

[5] B.K. Prasad, Can. Metall. Q. **51** (2), 210-220 (2013). DOI: https://doi.org/10.1179/1879139511Y.0000000030

[6] B. Unlu, Bull. Mater. Sci. **32** (4), 451-457 (2009). DOI: https://doi.org/10.1007/s12034-009-0066-0

[7] V. Ruusila, T. Nyyssonen, M. Kallio, P. Vuorinen, A. Lehtovaara, K. Valtonen, V.T. Kuokkala, Proc. Inst. Mech. Eng., Part J: J. Eng. Tribol. **227** (8), 878-887 (2013). DOI: https://doi.org/10.1177/1350650113478706.

[8] J.P. Pathak, S.N. Tiwari, Wear **155** (1), 37-47 (1992). DOI: https://doi.org/10.1016/0043-1648(92)90107-J

[9] Jan Gerkema, Wear **102** (3), 241-252 (1985). DOI: https://doi.org/10.1016/0043-1648(85)90222-4

[10] B. Unlu, E. Atik, J. Alloys Compd. **489** (1), 262-268 (2010). DOI: https://doi.org/10.1016/j.jallcom.2009.09.068

[11] B.K. Prasad, A.K. Patwardhan, A.H. Yegneswaran, Mater. Sci. Technol. **12** (5), 427-435 (1996). DOI: https://doi.org/10.1179/026708396790165885

[12] J.P. Pandey, B.K. Prasad, Metall. Mater. Trans. A. **29** (4), 1245-1255 (1998). DOI: https://doi.org/10.1007/s11661-998-0251-6

[13] S. Murphy, T. Savaskan, Wear **98**, 151-161 (1984). DOI: https://doi.org/10.1016/0043-1648(84)90224-2

[14] B.K. Prasad, Metall. Mater. Trans. A. **28** (3), 1245-1255 (1997). DOI: https://doi.org/10.1007/s11661-997-0067-9

[15] M. Aksoy, V. Kuzucu, H. Turhan, J. Mater. Process. Technol. **124** (1-2), 113-119 (2002). DOI: https://doi.org/10.1016/S0924-0136(02)00137-1

[16] A.W.J. De Gee, G.H.G. Vaessen, A. Begelinger, ASLE Transactions. **12** (1), 44-54 (2008). DOI: https://doi.org/10.1080/05698196908972245

[17] M. Nursoy, C. Oner, I. Can, Mater. Des. **29** (10), 2047-2051(2008). DOI: https://doi.org/10.1016/j.matdes.2008.04.020

[18] G. Cui, M. Niu, S. Zhu, J. Yang, Q. Bi, Tribol. Lett. **48** (2), 111-122 (2012). DOI: https://doi.org/10.1007/s11249-012-0007-8

[19] B.K. Prasad, J. Mater. Eng. Perform, **21** (10), 2155-2164 (2012). DOI: https://doi.org/10.1007/s11665-012-0139-x

[20] B. Juszczyk, J. Kulasa, S. Malara, M. Czepelak, W. Malec, B. Cwolek, L. Wierzbicki, Arch. Metall. Mater. **59** (2), 615-620 (2014). DOI: https://doi.org/10.2478/amm-2014-0101

[21] F. Summer, F. Grun, M. Offenbecher, S. Taylor, Tribol. Int. **131**, 238-250 (2019). DOI: https://doi.org/10.1016/j.triboint.2018.10.042

[22] M. Kestursatya, J.K. Jim, P.K. Rohatgi, Mater. Sci. Eng., A. **339** (1-2), 150-158 (2003). DOI: https://doi.org/10.1016/S0921-5093(02)00114-4